

Effect of hydro-thermal carbonisation on the structural properties of bulk-type wood (*Chamaecyparis obtusa*) upon high-temperature heat treatment

Seyoung Kim¹ · Hyun-uk Kim¹ · Young-hoon Seong¹ · Insub Han¹ · Sangkuk Woo¹ · Soo-hyun Kim¹

Published online: 10 July 2017
© Springer Science+Business Media, LLC 2017

Abstract Hydro-thermal carbonisation (HTC) is a method to convert biomorphic materials such as wood to carbon, with the advantage of enhancing their specific surface area to an extent greater than that by pyrolysis. In this study, wood samples underwent HTC at 250 °C, followed by a heat treatment at 600, 800 or 1000 °C. The cell walls of the HTC processed samples showed a structure made of alternating porous and dense carbon layers that changed as a function of the additional heat-treatment temperature. The specific surface area of the samples which underwent only a pyrolysis carbonisation drastically decreased at 80 °C, while that of the HTC samples was 473 m²/g, which enabled them to maintain a high-temperature stability. Compressive strength tests demonstrated plastic deformation and a different fracture mode for the HTC samples compared to the samples subjected to pyrolysis carbonisation only. Different values of mechanical strength in longitudinal and vertical directions were analysed.

Keywords Carbonisation · Pyrolysis · Mechanical properties · Heat treatment

1 Introduction

Carbonised wood has been widely applied for industrial purposes as the demand for charcoal has greatly increased with the growth of metal industries since the 1800s. In

recent times, through various researches on cellulose's decomposition kinetics, thermodynamics and by-products, carbonised wood has been used as activated carbon for various applications such as textiles, composite materials, filters and catalyst supports [1]. As the importance of the fine chemicals industry has been increasing in the world, there have been a great interest in and studies focusing on micro-reactor processes using activated carbon-supported precious metal catalyst [2]. Carbon supports can be manufactured in the form of powder, pellet or honeycomb, and used as a catalytic filter support or an absorbent. Catalysts such as Cu, Pd, Pt, Ir, Ru, Rh or Mn can be applied to it, and used for low-temperature selective catalytic reduction of NO or thermo-catalytic decomposition of methane for CO₂-free hydrogen production [3]. However, because carbonised wood has a lower specific surface area (SSA) than commercial activated carbon (400–1200 m²/g), it is difficult to commercialise [4]. Mohan et al. [5] obtained carbonised wood with SSA values of 2.04, 2.73, 25.4 and 1.88 m²/g by carbonising oak wood, pine wood, oak bark and pine bark at 400–450 °C, respectively. A recent breakthrough was when Yao et al. [6] carbonised Brazilian peppers, bamboo, sugar bagasse and hickory wood at 600 °C, and obtained SSA values of 234, 375.5, 388.3 and 401.0 m²/g, respectively, with optimised heat-treatment conditions [7].

One appropriate way to increase the surface area of carbonised wood is to use hydro-thermal carbonisation (HTC). Unlike thermal carbonisation that occurs in an inert gas, this thermo-chemical conversion is performed in water [8]. Raw wood and water are mixed and heated for the HTC process. The mixture evaporates at a subcritical temperature in the range 150–300 °C to generate water vapour pressure. From the generated water vapour pressure, the long hydrocarbon chains of cellulose, which is the main component of wood, are pyrolysed to finally yield a carbon-rich

✉ Seyoung Kim
saykim@kier.re.kr

¹ Energy Materials Laboratory, Korea Institute of Energy Research (KIER), 152 Gajeong-ro, Yuseong-gu, Daejeon, South Korea

solid [9, 10]. HTC is very effective in hydrolysing and dehydrating wood, generating hydro-char with high oxygenated functional groups, a precursor needed for producing activated carbon can be obtained [10, 11]. It was reported that excellent SSA characteristics were obtained for carbonised wood obtained by HTC using activating agents [12–15]. Such high SSA properties are very important for applications such as catalysis/electrolysis, separation of multi-sized molecules, energy storage in capacitors, electrodes of Li-ion batteries, CO₂ capture, and H₂ storage [16–22]. However, because such applications may operate also at high temperatures, research on carbonised wood properties at various temperature ranges is needed. In addition, most of the researches until now have focused on HTC yielding carbon particles or carbon powder and on their chemical properties. It is therefore hard to find research studies focusing on bulk wood of honeycomb type that can be applied to micro-reactors or on mechanical characteristics of HTC carbon which are required for industrialisation. The mechanical characteristics are important properties for support materials of catalyst and it also should be rigid enough for replacement or installation to system.

The purpose of this study is to investigate the changes in the geometrical and mechanical characteristics of bulk honeycomb type carbonised *Chamaecyparis obtusa* wood that has not been studied yet on mechanical strength obtained by HTC at 250 °C when it undergoes a further heat treatment process at different temperatures in nitrogen atmosphere.

2 Experimental

2.1 Carbonisation and sample preparation

Chamaecyparis obtusa (Japanese cypress, Hinoki) columnar samples with a square cross section and dimensions of 10 × 10 × 20 mm³ were prepared. The HTC process was conducted at 250 °C for 24 h in an autoclave with a 500 ml volume vessel. For each HTC process, ten samples were loaded together with water. The samples were then dried in an oven chamber at 120 °C for 24 h, and finally heat treated in nitrogen atmosphere at 600, 800 or 1000 °C. The temperature was increased with a heating rate of 5 °C/min. and kept for 60 min. Control samples were obtained by having the same raw materials undergoing only the pyrolysis

carbonisation process in nitrogen atmosphere. The HTC processed samples were named as HT and NT for heat treated samples in nitrogen.

Darcy's Law was applied on this carbonised honeycomb wood to measure its gas permeability. We obtained a value of 1.5×10^{-6} m³/s at a flow rate of 10 ml/s. It shows that a continuous flow of gas went through the carbonised wood honeycomb as not many perforation plates disturbed the gas flow through the vessel. Table 1 shows the heat treatment conditions and names of samples for each process.

2.2 Properties evaluation

Weight changes of the wood samples occurring during the hydrothermal carbonisation and nitrogen atmosphere heat treatment were measured using TGA (USA, TA instruments, SDT Q600). The microstructure and morphology of carbonised wood samples after each treatment were observed using a scanning electron microscope (SEM, Japan, Hitachi, S-4800). The sample dimensions were measured after each process using a micrometer, and changes in volume were determined using the mean value of the ten samples. The SSA, one of the main characteristics of HTC processed carbon, was measured by the Brunauer–Emmett–Teller (BET) method using N₂ gas at 77 K, and a Horvath–Kawazoe pore size distribution prediction and t-plot analysis were carried out as well.

Compression strength tests were conducted on samples of dimensions 10 × 10 × 20 mm³ using a universal testing machine (USA, Tinius Olsen, H10K-T) with a cross head speed of 1 mm/min. The samples were obtained by cutting different types of carbonised samples of original dimensions 20 × 20 × 40 mm³ before carbonisation. We particularly focused on the determination of the compression strength in both the longitudinal and vertical directions of the samples to observe the cell wall characteristics of the HTC processed carbon.

3 Results and discussion

The TGA results of the wood samples that underwent HTC and/or nitrogen pyrolysis carbonisation are shown in Fig. 1. For the HT samples, changes in weight after the HTC process (carried out at 250 °C), and after additional heat

Table 1 Heat treatment conditions and names of samples

Notation	NT600	NT800	NT1000	HT600	HT800	HT1000
HTC process temp. (°C)	–	–	–	250	250	250
Nitrogen process temp. (°C)	600	800	1000	600	800	1000

NT Nitrogen atmosphere carbonisation treatment (gas permeability 1.5×10^{-6} m³/s at 10 ml/s flow rate)

HT Hydrothermal carbonisation treatment

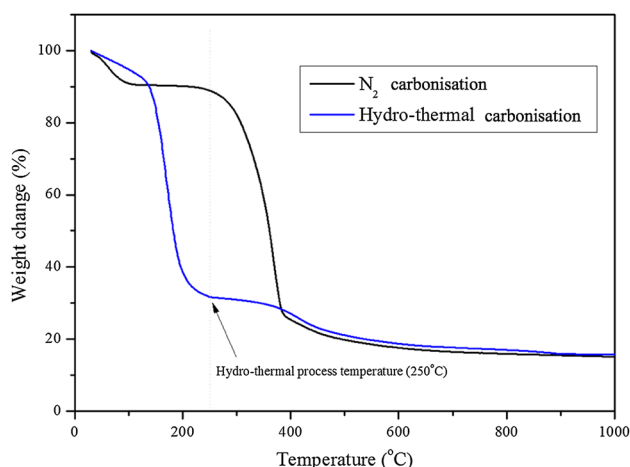


Fig. 1 TGA results of nitrogen and HTC process

treatment (at temperatures above 250 °C) were measured. For the NT samples, moisture evaporated at around 100 °C, and internal CO or CO₂ decomposed at 250 °C. Afterwards, thermal degradation of biomolecules occurred between 250 and 400 °C, and CO, H₂, and CO₂ decomposed and formed tar. It has been shown that hemicellulose decomposes at 200–400 °C, cellulose at 300–400 °C and lignin at 180–600 °C [23]. For HT sample, changes in weight during the HTC process were measured up to 250 °C, and heat treatment above 250 °C were measured in nitrogen atmosphere. HT samples decompose at relatively lower temperatures (180–200, 220, and 180–220 °C, respectively) during HTC because of the process conditions involving high vapour pressure [24]. Therefore, hydrolysis, dehydration, decarboxylation, aromatisation and recondensation are expected to occur between 130 and 250 °C during HTC, along with weight reduction [25]. However, after 400 °C, the carbon yields of NT and HT samples were similar and both gradually reduced with increasing temperature.

SEM observations of the cross section and surface microstructures of the NT and HT samples are shown in Fig. 2a, b. For the NT sample, formation of dense carbon was observed after the cell walls were carbonised. There was no significant change in the thickness of the cell walls with increasing carbonisation temperature. This is in agreement with the TGA results that indicated no significant change in weight after a carbonisation heat treatment at a temperature over 600 °C. In Fig. 2a, we could observe small particles on the surface of the NT samples. Their diameter gradually increased while their height decreased with increasing carbonisation temperature, thus enhancing the smoothness of the samples surface.

By contrast, HT samples exhibited after the HTC process a cell wall structure made of alternating porous and dense carbon layers as shown in Fig. 2b. A gradual

reduction in the thickness of the porous carbon layer was observed as the heat treatment temperature increased, while the thickness of the dense carbon layer inside the cell wall increased. The HT600 samples displayed a porous surface which showed gradual closing as the carbonisation heat treatment temperature increased, and for HT1000, most of the surface was a dense carbon layer. It has been shown that this phenomenon results from a recovery of the surface at high temperatures [26].

In addition, there were multiple cases of an unusual delamination phenomenon between porous and dense layers for the HT1000 samples, indicated with a white arrow in the bottom of Fig. 2b. For the HT samples, the volume shrinkage ratio and the coefficient of thermal expansion of porous and dense carbon layers are different from each other, inducing a residual stress during the heat treatment process in the carbonised structure. This residual stress reached a critical stress between 800 and 1000 °C, and the stress was released in form of delamination as shown in Fig. 2b.

The measurements of the volume shrinkage during the carbonisation process are shown in Fig. 3. The changes in volume as a function of the heat treatment temperature showed clear differences after the heat treatment at 1000 °C, namely that the NT sample shrunk more than the HT sample. The TGA results shown in Fig. 1 demonstrated the same final weight for both the HT and NT samples. The measured difference in their volumes indicates that the HT samples became less dense than the NT samples after carbonisation. These results are in agreement with the SEM observations of Fig. 2a, b showing porous layers. Despite Fig. 2b shows a gradual reduction of the porous layer thickness with increasing temperature, the volume reduction was still significantly lower for the HT samples because of the delamination that preserved from a thinning of the cell walls.

Nitrogen adsorption–desorption isotherms at 77 K for the HT samples are shown in Fig. 4. Except for a little hysteresis for the HT1000 samples, uniform micropore and mesopore characteristics without particular hysteresis were observed. Table 2 shows the estimated BET SSA and the total pore volume obtained from the nitrogen adsorption isotherms. Taking into consideration that the form of the nitrogen adsorption isotherms was consistent for all samples, it could be determined that the SSA and the total pore volume decreased with increasing heat treatment temperature. Given the previously reported measurements of volume change, this result was explained by a blocking of some pores while the overall structural framework kept its form. Furthermore, we estimated the micropore volume as a function of temperature by using the *t*-plot method. The micropore volume of the samples heat treated at 600 and 800 °C was about 48% of the total pore volume, and it was

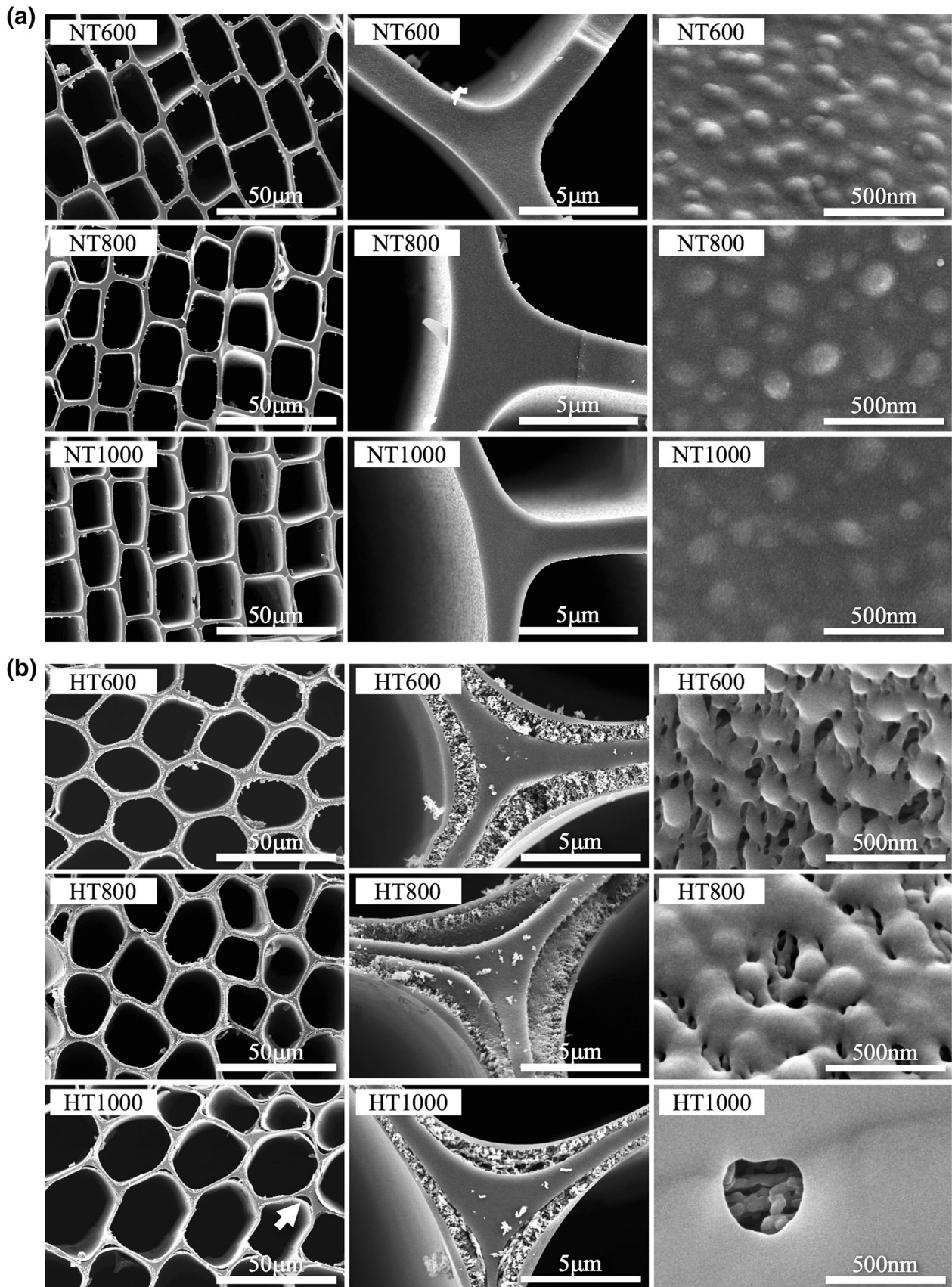


Fig. 2 a Cross section and surface SEM observation of NT sample. b Cross section and surface SEM observation of HT sample

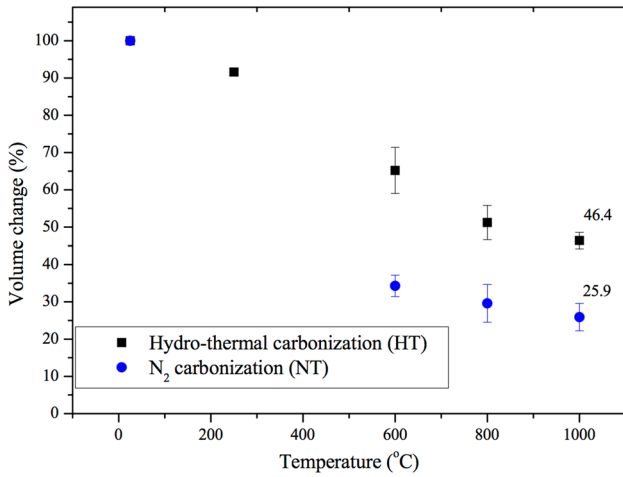


Fig. 3 Volume change result of nitrogen and HTC process

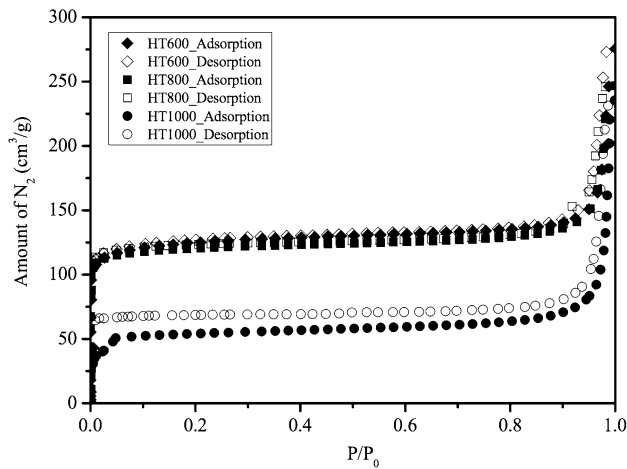


Fig. 4 Nitrogen adsorption-desorption isotherms of HT sample at 77 K

about 68% for samples heat treated at 1000 °C. Figure 5 shows the results of micropore size distribution using the

Horvath–Kawazoe method. The samples heat treated at 600 and 800 °C showed three distinct pore sizes comprised between 0.5 and 1.0 nm, while the samples heat treated at 1000 °C showed a small micropore volume at 0.6 nm pore size.

Nitrogen adsorption–desorption isotherms at 77 K for the NT samples showed different adsorption characteristics, notably a clear adsorption–desorption hysteresis for the NT800 and NT1000. This means that the samples did not have a uniform pore size and morphology. By contrast, the NT600 samples showed typical BET Type I adsorption isotherms, as shown in Table 2. Their SSA was 433 m²/g, and their total pore volume was 0.1910 cm³/g. The SSA of the NT600 samples was slightly smaller than that of the HT samples while their total pore volume was significantly smaller. This is due to the fact that 97% of the total pore volume of the NT samples was micropores, in contrast to the HT samples that had both micro- and mesopores. The NT800 samples exhibited a smaller SSA, indicating an increase in the carbonisation ratio and structural changes. On the other hand, the SSA and total pore volume of the HT800 samples were very similar to those of the HT600, suggesting that the structure of carbonised wood had been stabilised by the HTC process due to no structural change in high temperature comparing NT samples.

The results of compressive strength tests for the different samples are shown in Fig. 6a, b. The compressive strength tests were conducted in the longitudinal and vertical directions as shown in Fig. 6. The results show that the compressive strength improved in both directions as the carbonisation temperatures increased. For NT samples, the carbon structure converted to dense carbon due to decomposition of CO, H₂ and CO₂. The overall compressive strength of HT samples was lower due to their porous layers. However, as the proportion of dense layers thickness increased with increasing heat treatment temperature, the compressive strength increased accordingly.

The vertical compressive strength of the HT samples was very low, and did not significantly increase after a heat

Table 2 BET and pore volume of NT and HT samples

Samples	BET (m ² /g)	Total pore volume (cm ³ /g) at P/P ₀ =0.990	Micropore volume ^a (cm ³ /g)	Mesopore Volume ^b (cm ³ /g)	Percentage of micropore volume ^c (%)
NT600	433	0.1910	0.1860	0.005	97.4
NT800	174	0.1324	0.1074	0.025	81.1
NT1000	168	0.1036	0.0880	0.016	84.9
HT600	483	0.3891	0.1890	0.2001	48.6
HT800	473	0.3601	0.1716	0.1885	47.7
HT1000	208	0.1036	0.0702	0.0334	67.8

^aDetermined by t-plot analysis

^bMesopore volume = total pore volume – micropore volume

^cPercentage of micropore volume = micropore volume/total pore volume

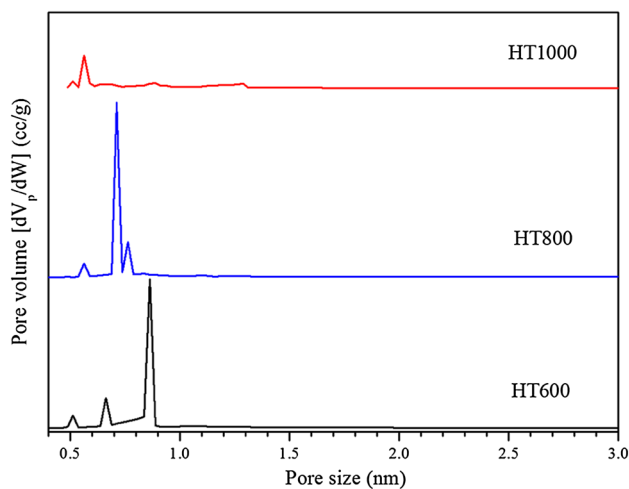


Fig. 5 The Horvath–Kawazoe pore size distribution of HT sample estimated from N₂ adsorption experiments at 77 K

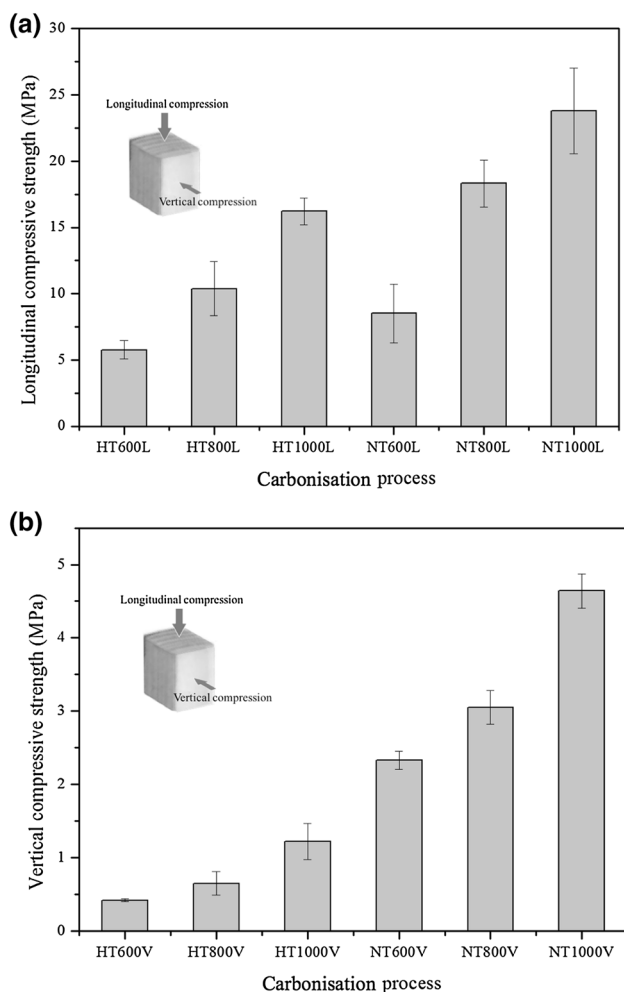


Fig. 6 **a** Longitudinal compressive strength result of NT and HT samples. **b** Vertical compressive strength result of NT and HT samples

treatment at higher temperatures. The cell walls are the part of carbonised wood that supports mechanical stress. Since those of the HT samples contain porous layers, a low value in the mechanical strength is unavoidable.

Figure 7 shows vertical compressive stress–displacement curves, which show very different results for the NT and HT samples. Under compressive stress, the NT samples exhibited brittle fracture behaviour similar to common carbon materials. In addition, the crushed sample shown in Fig. 7 displayed a crack with a clear brittle failure in the direction parallel to the load. On the other hand, the HT samples showed a typical ductile behaviour. The curves obtained for HT600 can be divided into three zones. The first one shows early elastic behaviour where cell walls supported the load and maintained the material structure. The curve is flat in the second zone; at this point, the cell walls had started being damaged by the compressive load and gradually stacked. Finally, the third zone shows a significant increase in the load, and corresponds to a situation in which all cell walls had been damaged and stacked [27]. No failure crack was observed for HT600, and only plastic deformation occurred. On the other hand, for HT800 and HT1000, a crack developed, leading to fracture at the end of the second zone. These brittle characteristics are due to carbon crystallization that started at temperatures above 600 °C.

4 Conclusion

In this study, HTC at 250 °C followed by an additional heat treatment at 600, 800 or 1000 °C under nitrogen was performed on wood samples. Their thermal stability along with their microstructural and mechanical properties after

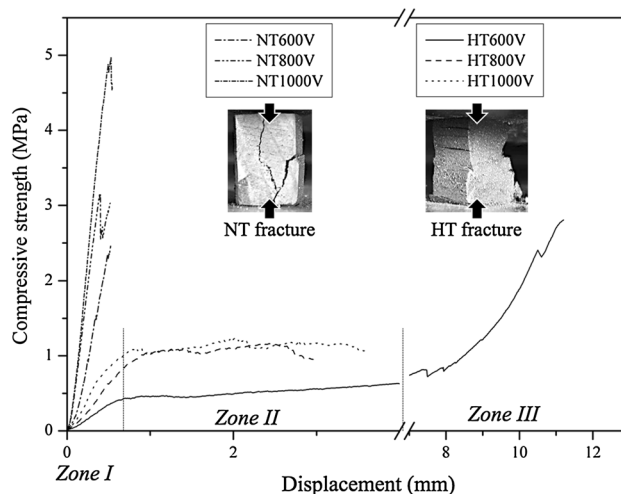


Fig. 7 Stress–displacement curve of vertical compression test

this carbonisation process were investigated. The TGA results for the HT (which underwent HTC process) samples were similar to those obtained with the NT samples (which underwent only the pyrolysis carbonisation under nitrogen). However, the HT samples were found to have a relatively porous structure with smaller (by 20%) volume shrinkage when heated at higher temperatures compared to that of the NT samples. Our SEM analysis showed a porous/dense carbon multi-layered structure for the HT samples. This structure explains their high specific surface area value of 483 m²/g found after the HTC. When an additional heat treatment was conducted, a value as high as 473 m²/g was still maintained up to 800 °C. Furthermore, it was found that both meso and micropores existed in the HT samples. In terms of mechanical properties, the HTC process reduced the brittleness of the carbonised wood material which exhibited large plastic deformation. Also, it was found out that failure due to compressive stress was not caused by crack generation as in common carbon.

In conclusion, the structural changes observed in our wood samples during the HTC process ensured their stability when exposed to heat treatments at high temperatures. They furthermore exhibited high specific surface area values and plastic deformation during mechanical loading.

Acknowledgements This work was conducted under the framework of the research and development program of the Korea Institute of Energy Research (B6-2490).

References

1. C.E. Byrne, D.C. Nagle, *Carbon* **35**, 259–266 (1997)
2. E. Auer, A. Freund, J. Pietsch, T. Tacke, *Appl. Catal. A* **173**, 259–271 (1998)
3. J.M. Gatica, A.L. García-Cabeza, M.P. Yeste, R. Marín-Barrios, J.M. González-Leal, G. Blanco, G.A. Cifredo, F.M. Guerra, H. Vidal, *Chem. Eng. J.* **29**, 174–184 (2016)
4. T.X. Fan, T. Hirose, T. Okabe, D. Zhang, *J. Porous Mater.* **8**, 3 (2001)
5. D. Mohan, C.U. Pittman Jr., M. Bricka, F. Smith, B. Yancey, J. Mohamed, P.H. Steele, M.F. Alexandre-Franco, V. Gomez-Serrano, H. Gong, *J. Colloid Interface Sci.* **310**, 57–73 (2007)
6. Y. Yao, B. Gao, H. Chen, L. Jiang, M. Inyang, A.R. Zimmerman, X. Cao, L. Yang, Y. Xue, H. Li, *J. Hazard. Mater.* **209–210**, 408–413 (2012)
7. D.C. Cruz, Thesis, University of Western Ontario, December 2012
8. A. Jain, R. Balasubramanian, M.P. Srinivasan, *Chem. Eng. J.* **283**, 789–805 (2016)
9. M. Sevilla, A.B. Fuertes, *Chem. Eur. J.* **15**, 4195–4203 (2009)
10. M. Sevilla, A.B. Fuertes, *Carbon* **47**, 2281–2289 (2009)
11. M. Sevilla, A. Fuertes, R. Mokaya, *Energy Environ. Sci.* **4**, 1400–1410 (2011)
12. A. Romero-Anaya, M. Ouzzine, M. Lillo-Ródenas, A. Linares-Solano, *Carbon* **68**, 296–307 (2014)
13. L. Wang, Y. Guo, B. Zou, C. Rong, X. Ma, Y. Qu, Y. Li, Z. Wang, *Bioresour. Technol.* **102**, 1947–1950 (2011)
14. Z. Zhang, Y. Qu, Y. Guo, Z. Wang, X. Wang, *Colloids Surf. A* **447**, 183–187 (2014)
15. C. Falco, J.M. Sieben, N. Brun, M. Sevilla, T. van der Mauelein, E. Morallón, D. Cazorla-Amorós, M.M. Titirici, *Chem. Sus. Chem.* **6**, 374–382 (2013)
16. C. Pham-Huu, C. Bouchy, T. Dintzer, G. Ehret, C. Estournes, M.J. Ledoux, *Appl. Catal. A* **180**, 385–397 (1999)
17. A. Jain, V. Ong, S. Jayaraman, R. Balasubramanian, M. Srinivasan, *J. Supercrit. Fluid* **107**, 513–518 (2016)
18. M. Biswal, A. Banerjee, M. Deo, S. Ogale, *Energy Environ. Sci.* **6**, 1249–1259 (2013)
19. P. Simon, Y. Gogotsi, *Nat. Mater.* **7**, 845–854 (2008)
20. H.L. Wang, Z. Li, J.K. Tak, C.M.B. Holt, X.H. Tan, Z.W. Xu, B.S. Amirkhiz, D. Hayfield, A. Anyia, T. Stephenson, D. Mitlin, *Carbon* **57**, 317–328 (2013)
21. V. Aravindan, J. Sundaramurthy, A. Jain, P.S. Kumar, W.C. Ling, S. Ramakrishna, M.P. Srinivasan, S. Madhavi, *Chem. Sus. Chem.* **7**, 1858–1863 (2014)
22. A.C. Lua, J. Guo, *Langmuir* **17**, 7112–7117 (2001)
23. H. Hofbauer, M. Kaltschmitt, T. Nussbaumer, *Energie aus Biomasse* (Springer, Berlin, 2009), pp. 375–406
24. O. Bobleter, *Prog. Polym. Sci.* **19**, 797–841 (1994)
25. W.S.L. Mok, M.J. Antal, P. Szabo, G. Varhegyi, B. Zelei, *Ind. Eng. Chem. Res.* **31**, 1162–1166 (1992)
26. J.M. Kim, I. S. Song, D. Cho, I. Hong, *Carbon Lett.* **12**, 131–137 (2011)
27. G. Lu, G.Q. Lu, Z.M. Xiao, *J. Porous Mater.* **6**, 4 (1999)